Semnan University

Mechanics of Advanced Composite Structures

Journal homepage: https://macs.semnan.ac.ir/

ISSN: 2423-7043

Research Article

Advancing Sustainable Mobility Through Hybrid Kenaf–Cenosphere Reinforced Epoxy Composites: Integrated Assessment of Mechanical Performance, Lightweighting, Sustainability, and Cost Efficiency

Chandrika S* **and T R Veena**

Department of Industrial Engineering and Management, Siddaganga Institute of Technology, Tumakuru 572103, Karnataka, India

ARTICLE INFO

Article history:

Received:
Revised:
Accepted:

Keywords:

Natural Fiber Reinforcement;
Lightweight Structures;
Syntactic Fillers;
MADM;
TOPSIS.

ABSTRACT

Kenaf–Cenosphere hybrid epoxy composites were fabricated via hand lay-up followed by compression moulding to investigate the effect of waste-derived hollow Cenosphere on the physical, mechanical, lightweighting, and sustainability characteristics of natural fibre-reinforced composites for mobility applications. Composites were prepared with constant kenaf fiber content (35 wt.%) and varying Cenosphere content from 0–15 wt.%: C1 (0 wt.%), C2 (5 wt.%), C3 (10 wt.%), and C4 (15 wt.%), with epoxy content adjusted accordingly. Increasing Cenosphere content reduced theoretical density from 1.28 to 1.22 g/cm^3 and decreased actual density by 6.5%, while void content increased from 3.9% to 5.7%. Water absorption decreased by 26.2%, indicating improved moisture resistance. Mechanical analysis showed that tensile and flexural strengths reached maximum values of 45.6 MPa and 88.9 MPa for C3, representing improvements of 39% and 13.2%, respectively, over the control composite. Impact strength increased continuously, reaching 15.6 kJ/m^2 for C4, corresponding to a 59.2% enhancement. Lightweighting analysis demonstrated significant weight reductions of 84.33–85.35% relative to mild steel and 54.44–57.41% compared to aluminum. Sustainability assessment indicated improved environmental performance with increasing Cenosphere content due to higher industrial waste utilization, reduced epoxy dependence, and renewable kenaf incorporation, yielding a ranking of C4 > C3 > C2 > C1. SEM analysis revealed improved fiber–matrix adhesion for C3 and enhanced crack branching in C4. TOPSIS analysis ranked C3 and C4 as the most preferred configurations (relative closeness = 0.59). Overall, C3 provided the best balance between mechanical performance, lightweighting, cost efficiency, and sustainability, while C4 was more suitable for impact-resistant applications.

1. Introduction

Polymer composites have emerged as a critical class of engineering materials due to their excellent strength-to-weight ratio, design flexibility, and adaptability across a wide range of applications, including aerospace, automotive, marine, and construction industries [1], [2]. The growing demand for lightweight, high-performance, and environmentally sustainable materials has driven the development of hybrid composite systems that integrate natural fibers with industrial waste-derived fillers [3], [4], [5]. Such composites not only meet rigorous

* **Corresponding author.**
E-mail address: chandrikaim012@gmail.com

Cite this article as:
Chandrika, S., Veena T R., 2026. Title of article. *Mechanics of Advanced Composite Structures*, 13(2), pp. xxx-xxx.
https://doi.org/10.22075/MACS.2025.39313.2050

performance requirements but also support resource efficiency, reduce reliance on non-renewable materials, and align with circular economy principles. By leveraging the complementary properties of different reinforcements, hybrid composites provide a versatile platform for balancing mechanical, thermal, and functional performance while addressing environmental concerns [6].

Recent studies have reported significant advancements in the development of natural fiber-reinforced and hybrid polymer composites for structural and semi-structural applications [5], [7], [8]. Hybridization of natural fibers with secondary reinforcements such as particulate fillers and synthetic fibers has been widely explored as an effective strategy to enhance mechanical performance, reduce density, and improve functional properties [9], [10], [11]. These approaches have demonstrated improvements in tensile strength, flexural behavior, and impact resistance due to synergistic interactions between fibers and fillers, which contribute to improved stress transfer and crack-bridging mechanisms. In particular, recent research has highlighted the role of filler modification and hybrid reinforcement architectures in optimizing composite performance for lightweight engineering applications. The incorporation of particulate reinforcements in polymer matrices has been shown to enhance stiffness and dimensional stability while maintaining acceptable toughness. Furthermore, sustainable composite development using agricultural waste-based fibers and industrial by-product fillers has gained increasing attention due to environmental concerns and the need for circular economy-based material solutions [12], [13], [14], [15].

Among natural fibers, kenaf (Hibiscus cannabinus) has received considerable attention due to its abundance, biodegradability, renewability, low density, and relatively high specific strength [16], [17], [18]. These characteristics make kenaf fibers suitable alternatives to conventional synthetic fibers, such as glass, particularly in semi-structural applications where weight reduction is crucial. Despite their advantages, natural fibers exhibit limitations, including a hydrophilic nature and limited thermal stability, which can compromise fiber–matrix interfacial bonding and long-term mechanical performance. Various strategies, including chemical surface treatments and hybridization with secondary reinforcements, have been explored to enhance interfacial adhesion, reduce moisture absorption, and broaden the application range of natural fiber composites[19], [20], [21].

In parallel, Cenosphere-lightweight, hollow aluminosilicate microspheres derived as byproducts from coal-fired thermal power plant fly ash have gained recognition as sustainable fillers for polymer composites. Their low density, high compressive strength, and thermal stability make them effective for enhancing stiffness, dimensional stability, and impact energy absorption while reducing overall composite weight. Additionally, the use of Cenosphere addresses environmental concerns by providing a value-added route for fly ash utilization. When used in polymer matrices, Cenosphere can improve hardness and impact toughness, although excessive filler loading may introduce brittleness due to particle agglomeration and stress concentration [22], [23], [24].

Epoxy resin is widely employed as a polymer matrix for structural composites owing to its excellent adhesion, chemical resistance, and low curing shrinkage. However, neat epoxy is inherently brittle and exhibits poor impact resistance, limiting its application in dynamic or impact-prone environments [25], [26]. Single-phase reinforcement, either natural fibers or particulate fillers, often improves specific properties but introduces performance trade-offs. For example, natural fibers enhance tensile and flexural strengths but provide limited improvement in hardness and impact toughness, whereas Cenosphere improves stiffness and energy absorption but can reduce static strength at higher concentrations [27].

These challenges highlight the need for a hybrid reinforcement strategy that combines the tensile and flexural benefits of natural fibers with the stiffness and impact energy absorption provided by Cenosphere. Hybrid kenaf/Cenosphere composites have the potential to achieve a balanced combination of mechanical, physical, and functional properties while maintaining lightweight and sustainable characteristics. Despite the promising potential, systematic studies on the synergistic effects of kenaf fibers and Cenosphere in epoxy matrices-particularly focusing on the interplay between density, void content, water absorption, tensile, flexural, and impact performance remain limited.

The developed composite system offers environmental benefits through the synergistic use of renewable natural fibers and industrial waste-derived fillers. Kenaf fibers represent a sustainable reinforcement material because they are renewable, biodegradable, rapidly renewable, and require comparatively lower energy for production than synthetic fibers[28]. The replacement of synthetic reinforcements with natural fibers can potentially reduce energy consumption and associated carbon emissions during material manufacturing.

UNCORRECTED PROOF

Cenospheres are hollow aluminosilicate particles recovered from fly ash generated during thermal power plant operations. Their utilization promotes waste valorisation by converting industrial by-products into useful engineering materials rather than directing them to landfills. Furthermore, their low-density nature contributes to lightweight composite structures, which can potentially improve fuel efficiency and reduce energy consumption in transportation applications. Therefore, the integration of kenaf fibers and Cenosphere supports sustainable material development through renewable resource utilization, waste reduction, and improved material efficiency.

Selecting a substance based on prior experience or trial and error often works. The process of choosing the right material is costly and time-consuming, and it is seen as a component of the design process [29]. For a given application, several materials are typically appropriate, and the final choice requires trade-offs. Along with this, there are certain benefits and drawbacks [30].

It is very difficult or even impossible to choose the right material when using a design approach like Design of Experiments (DOE). Additionally, it may result in the omission of numerous possible materials throughout the design cycle [31]. Over the years, many systematic approaches to material selection have been put forth in an effort to get around these issues and improve the design process's efficacy and efficiency. The positive and negative ideal solutions are defined by the TOPSIS technique. If the alternative is closer to the positive ideal solution and farther from the negative ideal solution, it is deemed the best answer. TOPSIS is simple to use, and even when features are added, the overall number of stages in the process stays the same [32].

The present study addresses the limited systematic investigation of hybrid kenaf fiber and Cenosphere-filled epoxy composites, particularly with respect to the combined effects of particulate–fiber reinforcement on mechanical performance, density reduction, and suitability for sustainable mobility applications. While previous studies have primarily focused on either natural fiber reinforcement or particulate fillers independently, limited work has explored their synergistic integration and its influence on specific mechanical properties and lightweight efficiency.

The outcomes of this work are expected to provide a comprehensive understanding of hybrid natural fiber–Cenosphere composites and guide their design for lightweight, sustainable, and impact-resistant applications.

2. Methods and Materials

2.1. Materials

Fig. 1. Raw materials used in the development of the composite: (a) Kenaf mat; (b) Epoxy matrix; and (c) Cenosphere.

Figure 1 presents the raw materials used in the present study for the preparation of composites. The matrix material used in this study was epoxy resin (Lapox L12) along with K-6 hardener, owing to its superior adhesion, chemical resistance, and dimensional stability. Kenaf fibers were selected as the fibrous reinforcement because of their favourable strength-to-weight ratio and sustainability; prior to incorporation, the fibers were subjected to alkali treatment in order to remove surface impurities and enhance interfacial bonding with the epoxy matrix. Cenospheres, obtained as a byproduct from industrial fly ash, were employed as the particulate filler. These hollow alumina-silicate microspheres were sieved to an average particle size of 75 µm to ensure uniform dispersion within the resin. The combined use of kenaf fibers and Cenospheres was aimed at developing hybrid composites with tailored mechanical properties and reduced density.

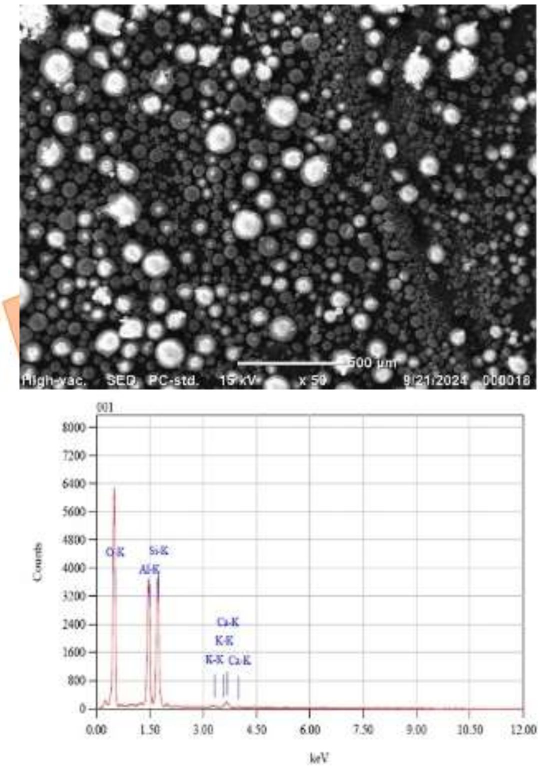

Fig. 2. SEM image of Cenospheres and their EDS spectra

Figure 2 shows the scanning Electron Microscopy (SEM) image of Cenospheres and their EDS spectra. The SEM micrograph reveals the characteristic spherical morphology of the Cenospheres, which are hollow aluminosilicate microspheres formed during coal combustion. The particles appear as smooth, discrete, and uniformly distributed spheres with varying diameters ranging from a few micrometers to several hundred micrometers. The presence of mostly intact, closed spheres indicates good structural integrity, while occasional broken or irregular particles suggest thin-walled Cenospheres that may have fractured during processing. The overall distribution highlights a porous and lightweight structure, making Cenospheres suitable for syntactic foam and lightweight composite applications.

The corresponding EDS spectrum confirms the chemical composition of the Cenospheres. The major peaks correspond to oxygen (O), silicon (Si), and aluminium (Al), which are typical constituents of aluminosilicate glassy phases. Minor peaks of calcium (Ca) and potassium (K) are also observed, reflecting the presence of trace oxides such as CaO and K_2O in fly ash-derived Cenospheres. The dominance of Si, Al, and O indicates that the Cenospheres are primarily composed of silica (SiO_2) and alumina (Al_2O_3), while the minor elements contribute to the heterogeneity of the shell composition.

The combination of SEM and EDS confirms that the Cenospheres exhibit a spherical hollow morphology with a chemical composition dominated by aluminosilicate phases. These features make them lightweight, thermally stable, and suitable as fillers in polymer, metal, and ceramic matrices for weight reduction, thermal insulation, and enhanced mechanical performance.

2.2. Composite Fabrication

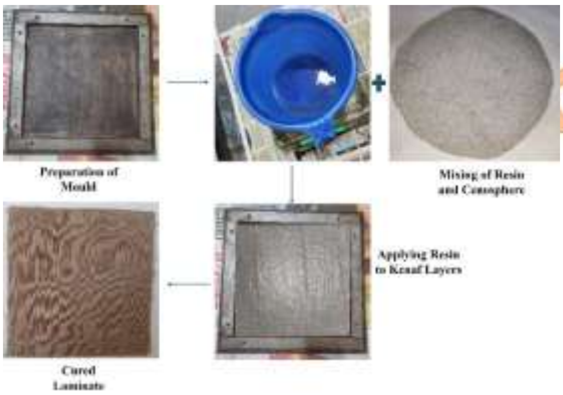

Fig. 3. Steps involved in preparation of composite laminate.

Figure 3 presents the steps involved in the preparation of composite laminates. In the present work, four different composite configurations were developed by systematically varying the Cenosphere content while keeping the kenaf fiber reinforcement constant at 35 wt.% in the form of three layers. The first configuration (Sample 1) consisted of 35 wt.% kenaf fibers and 65 wt.% epoxy without any Cenosphere addition, serving as the reference baseline for comparison. In the second configuration (Sample 2), 5 wt.% Cenospheres were incorporated into the epoxy matrix, reducing the epoxy content to 60 wt.% while maintaining the kenaf reinforcement constant. The third configuration (Sample 3) contained 10 wt.% Cenospheres with 55 wt.% epoxy and 35 wt.% kenaf fibers. Finally, the fourth configuration (Sample 4) was developed with the highest filler content, i.e., 15 wt.% Cenospheres, along with 50 wt.% epoxy and 35 wt.% kenaf fibers. This systematic variation in Cenosphere content was designed to evaluate the influence of increasing particulate reinforcement on the mechanical performance of kenaf fiber-reinforced epoxy composites, while maintaining a consistent fiber volume fraction across all specimens.

The fabrication of kenaf-Cenosphere reinforced epoxy composites was carried out using the hand lay-up method followed by compression molding to ensure uniform consolidation and surface finish. Initially, the epoxy resin (Lapox L12) and K-6 hardener were mixed in the manufacturer-specified stoichiometric ratio and stirred thoroughly to obtain a homogeneous mixture. Cenospheres, sieved to an average particle size of 75 µm, were gradually introduced into the epoxy resin at different weight fractions corresponding to the sample configurations described. The mixture was mechanically stirred for 20–25 minutes to achieve uniform dispersion of Cenospheres and to minimize particle agglomeration. Kenaf fibers were prepared in the form of three layers with a total reinforcement of 35 wt.% for all composites.

For composite preparation, a mold coated with a thin layer of release agent was employed. The prepared kenaf fiber layers were placed sequentially within the mold cavity, and the Cenosphere-epoxy mixture was poured uniformly over them to ensure complete impregnation. Gentle hand rolling was carried out to remove entrapped air bubbles and promote wetting of the fibers. The lay-up was then subjected to compression moulding at a pressure of 0.5–1 MPa for 24 hours at room temperature to facilitate initial curing. Post-curing was subsequently performed at 80 °C for 2 hours in a hot-air oven to ensure complete crosslinking of the epoxy matrix and to enhance the thermal and mechanical stability of the composites. The fabricated laminates were demoulded and cut into specimens of required dimensions using a diamond saw in accordance with ASTM standards for tensile, flexural, impact, and hardness testing. Table 1 lists the specifics of the suggested composites.

Table 1. Composite configuration

Composite Configuration	Cenosphere (wt%)	Kenaf (wt. %)	Epoxy (wt.%)
C1	0	35	65
C2	5	35	60
C3	10	35	55
C4	15	35	50

The prepared composite laminates are presented in Figure 4.

Fig. 4. Prepared composite laminates

2.3. Physical Characterization

The density and water absorption capacity of the suggested composites are ascertained through physical characterisation. Density, which is determined using the conventional relationship between density, mass, and volume as demonstrated in Eq. 1, is one of the most crucial considerations when choosing a material for a particular technological application.

$$Density = {}^{Mass}/_{Volume} \qquad (1)$$

Using the ASTM D 570-98 standard, the composite's response to water absorption is assessed. The water absorption % is calculated using Equation 2.

$$Water\ absorption\ (\%) = \left(\frac{w_f - w_i}{w_i}\right) \times 100 \qquad (2)$$

where w_i is the sample's initial weight and w_f is its final weight after the test.

The 76 mm x 25 mm samples are weighed using an advanced weighing scale apparatus prior to being immersed in water. After that, they are immersed in water, and at 2, 6, 12, 24, 36, 48, and 72 hours, their weights are recorded using the same advanced weighing scale apparatus.

2.4. Mechanical Characterization

All mechanical tests were performed at room temperature and laboratory ambient conditions. Test specimens were prepared from molded panels according to the relevant ASTM geometry and finished by machining or sawing to the required dimensions. Figure 5 shows the testing arrangements used for mechanical characterization.

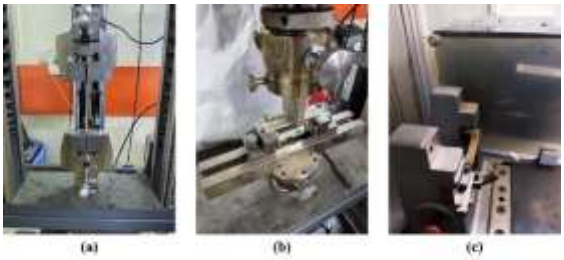

Fig. 5. Testing arrangements for (a) Tensile testing; (b) Flexural testing and (c) Charpy impact testing

Tensile properties of the composites were evaluated as per ASTM D3039 using a computer-controlled universal testing machine (UTM) equipped with a suitable load cell. Rectangular flat coupons were prepared to the standard dimensions, and the specimen width and thickness were measured precisely using a digital micrometer. Specimens were mounted in wedge grips, ensuring proper alignment to prevent eccentric loading. The tests were conducted under displacement control at a crosshead speed of 2 mm/min, as recommended by the standard. Load–displacement data were recorded continuously, and the tensile strength, modulus, and failure strain were calculated. Five specimens were tested for each composition, and the average values were reported.

Flexural strength and modulus were determined in accordance with ASTM D790 using a three-point bending setup on the universal testing machine. Rectangular specimens were prepared and placed on two supports with a span-to-depth ratio of 16:1, as prescribed by the standard. A loading nose applied force at the midpoint of the span at a constant crosshead speed, selected based on specimen thickness to maintain the recommended strain rate. Load–deflection data were recorded until fracture or the specimen reached the maximum deflection limit. Flexural strength was calculated from the maximum load using standard formulas, and the flexural modulus was obtained from the slope of the initial linear region of the load–deflection curve. For each formulation, a minimum of five specimens were tested, and mean values with standard deviation were reported.

The impact behaviour of the composites was evaluated using a Charpy impact tester in accordance with ASTM D6110. Rectangular specimens of standard dimensions were prepared. The specimens were positioned horizontally as a simple beam, supported at both ends, with the notch facing away from the striking pendulum. During testing, the pendulum was released from a fixed height and impacted the specimen at the centre of the span. The energy absorbed in breaking the specimen was measured directly by the tester as the difference between the initial and final heights of the pendulum swing. Charpy impact strength was then calculated by normalizing the absorbed energy with respect to the specimen's cross-sectional area at the notch. A minimum of five specimens for each composite composition were tested to ensure repeatability, and the average values with standard deviation were reported. Fractured surfaces were visually examined to identify the mode of failure, such as brittle fracture, fiber pull-out, or matrix cracking.

2.5. MADM and TOPSIS

A branch of operations research called multi-attribute decision making (MADM) thoroughly assesses a number of competing criteria when making decisions. Multiple criterion problem solving, planning, and structuring are related to MADM. The goal of MADM is to assist decision-makers who are having trouble choosing the optimal option from the range of options. Usually, there is no such thing as a unique optimal solution, and in order to distinguish amongst the options, the decision maker's preferences must be used.

The four distinct polymeric composite configurations are chosen for this study, and their experimentally assessed mechanical and physical characteristics are taken into account. The decision matrix is created, and the evaluation indices are established. The best option from the list is chosen using the Technique for Order of Preference by Similarity to Ideal Solution (TOPSIS).

TOPSIS is a methodical statistical tool that helps select the optimal choice from all of the options provided and has been successfully applied in a variety of application areas [33]. According to the TOPSIS approach, an option is considered ideal if it is the one that is farthest away from the negative ideal solution (NIS) and closest to the positive ideal solution (PIS). Values representing the best and worst outcomes for each of the criteria under consideration make up PIS and NIS. The TOPSIS process starts by creating a payoff matrix that includes all of the criteria and assigning weights, either subjective or objective, to each one. While the objective weights are determined using the entropy approach, the subjective weights are determined by decision makers.

Each criterion is linked to a cost or benefit idea. Smaller values are chosen when the cost criterion is included, but the greatest value is preferred when the benefit criterion is present. The decision matrix is further normalized for comparison purposes, and a weighted normalization matrix is subsequently created using the weights derived from the entropy technique. Calculating PIS and NIS is the next stage, after which the separation measure from PIS and NIS is calculated. The ranking of the alternatives is determined by determining their relative proximity to both PIS and NIS. The following lists the steps in the TOPSIS methodology:

Step 1- Normalization of the decision matrix: The decision matrix is normalized using the normalised vector "r_{ij}," which is determined using Equation 3.

$$r_{ij} = \frac{x_{ij}}{\sqrt{\sum_{i=1}^{m} x_{ij}^2}} \tag{3}$$

where, i = 1, 2,....., m and j = 1,2,....,n

Step 2- Weight determination: The weights for each criterion are determined using the entropy approach. The proportion "P_{ij}" of the index is determined using Equation 4, while the entropy E_j of index j is determined using Equation 5.

$$P_{ij} = \frac{x_{ij}}{\sum_{i=1}^{m} x_{ij}} \tag{4}$$

$$E_j = -k \sum_{i=1}^{m} P_{ij} \, x \, ln \, P_{ij} \tag{5}$$

where k is given by Eq. 6

$$k = {}^{1}/_{\ln m} \tag{6}$$

where m stands for the alternatives that were employed in the study (in this case, m=4).

The weight "w_j" for each criterion is calculated using Eq. 7

$$w_j = \frac{[1 - E_j]}{\sum_{j=1}^{n} [1 - E_j]} \tag{7}$$

Step 3-Calculation of the standardized weight value (v_{ij}): "v_{ij}" is found using Eq. 8, which aids in the creation of a weighted normalised matrix.

$$v_{ij} = w_j r_{ij} \tag{8}$$

where, i = 1, 2,....., m and j = 1, 2,....,n

Step 4- Determine the positive and negative ideal solution: The positive and negative ideal solution is determined using Eq. 9 and Eq. 10, respectively.

$$A^{+} = \{(\max_i v_{ij}, j\epsilon J_1), (min_i v_{ij,} j\epsilon J_2), i = 1,2,\dots,m\} = v_1^{\#}, v_2^{\#}, \dots, v_n^{\#} \quad (9)$$

$$A^{-} = \{(\min_i v_{ij}, j\epsilon J_1), (max_i v_{ij,} j\epsilon J_2), i = 1,2,\dots,m\} = v_1^{\wedge}, v_2^{\wedge}, \dots, v_n^{\wedge} \quad (10)$$

Step 5-Calculation of separation measures: The separation from PIS and NIS and relative closeness are calculated using Eq. 11, Eq. 12, and Eq. 13, respectively.

$$S^{\#} = \sqrt{\sum_{j=1}^{n} (v_{ij} - v_j^{\#})^2} \quad (11)$$

$$S^{\wedge} = \sqrt{\sum_{j=1}^{n} (v_{ij} - v_j^{\wedge})^2} \quad (12)$$

$$C_i^{*} = \frac{S_i^{\wedge}}{(S_i^{\#} + S_i^{\wedge})} \quad (13)$$

Relative closeness will be in the range of 0 to 1. When C_i^{*} = 0, $A_i = A^{+}$, which means that A_i is the most optimal evaluation objective. Based on C_i^{*}, evaluation objectives are sorted from largest to smallest, and the objective with the largest C_i^{*} is the best objective of all the alternatives.

Step 6-Ranking the priority based on descending value of C_i^{*}: The larger index value means better performance of the alternatives.

2.6. Lightweighting Analysis

Lightweighting analysis was conducted to evaluate the potential of the developed kenaf–Cenosphere reinforced epoxy composites as substitutes for conventional metallic materials used in automotive applications. The actual density values obtained experimentally were used to determine the percentage weight reduction achievable relative to commonly employed automotive materials, namely mild steel and aluminium.

The percentage weight reduction was calculated using Eq. 14:

$$Weight\ Reduction(\%) = \frac{\rho_{reference} - \rho_{composite}}{\rho_{reference}} \times 100 \quad (14)$$

where, $\rho_{reference}$ is the density of the conventional material (steel or aluminium), $\rho_{composite}$ is the actual density of the developed composite.

For comparison, the densities of mild steel and aluminium were considered as 7.85 g/cm^3 and 2.70 g/cm^3, respectively. The analysis assumes equal-volume replacement of metallic components with composite materials, which is a commonly adopted approach in lightweight structural assessments for transportation applications.

2.7. Sustainability Assessment

A sustainability assessment was conducted to evaluate the environmental benefits associated with the incorporation of kenaf fibers and Cenospheres in the epoxy matrix. The analysis focused on three key sustainability indicators: (i) density reduction, (ii) utilization of industrial waste materials, and (iii) incorporation of renewable natural fibers.

The density reduction achieved by each composite formulation was calculated relative to the control composite (C1), which contained no Cenosphere reinforcement. The percentage density reduction was determined using Eq. 15.

$$Density\ Reduction(\%) = \frac{\rho_{C1} - \rho_i}{\rho_{C1}} \times 100 \quad (15)$$

where, ρ_{C1} is the density of the control composite, ρ_i is the density of the respective Cenosphere-filled composite.

In addition to density reduction, the sustainability contribution of Cenospheres was assessed based on their origin as industrial by-products generated from coal-fired thermal power plants. Their incorporation into polymer composites enables waste valorisation and reduces the requirement for virgin raw materials. Similarly, kenaf fiber reinforcement was evaluated from the perspective of renewability, biodegradability, and reduced embodied energy relative to conventional synthetic reinforcements.

Based on these considerations, a comparative sustainability ranking of the developed composites was established by considering lightweighting potential, waste utilization, and renewable material content.

3. Results and Discussions

Table 2 shows a bird's-eye perspective of the acquired data during the physio-mechanical characterisation of the suggested composites.

Table 2. Consolidated list of results

Composite	Theoretical Density (g/cm^3)	Actual Density (g/cm^3)	Void Content (%)	Water Absorption (%)	Tensile Strength (MPa)	Flexural Strength (MPa)	Impact Strength (kJ/m^2)
C1	1.28	1.23	3.9	4.2	32.8	78.5	9.8
C2	1.26	1.21	4.0	3.8	42.1	85.7	11.4
C3	1.25	1.19	4.8	3.5	45.6	88.9	13.2
C4	1.22	1.15	5.7	3.1	38.3	79.4	15.6

3.1. Density

The variation in density is presented in Figure 6.

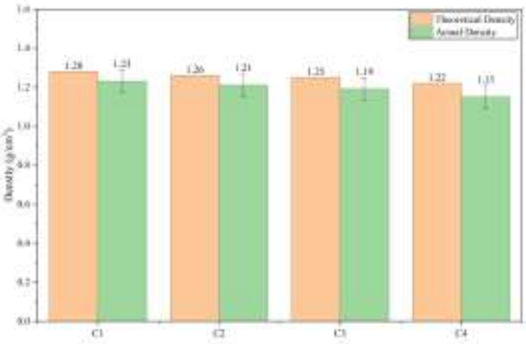

Fig. 6. Variation in density of developed composites

The theoretical density of the composites exhibited a progressive decrease from 1.28 g/cm^3 for C1 to 1.22 g/cm^3 for C4 as the Cenosphere content increased. This trend is consistent with expectations based on material properties, since Cenospheres are hollow aluminosilicate microspheres with very low intrinsic density compared to epoxy resin. As epoxy, the relatively heavier constituent, is gradually substituted by Cenospheres, the overall mass per unit volume of the composite reduces in accordance with the rule of mixtures. This indicates that filler incorporation effectively lowers the density, making the material more lightweight-an important attribute for structural and transportation applications.

The actual density values showed a similar decreasing trend, dropping from 1.23 g/cm^3 (C1) to 1.15 g/cm^3 (C4). However, the magnitude of reduction in actual density was sharper than that predicted by theoretical calculations, which resulted in a steady rise in void content from 3.9% at C1 to 5.7% at C4. This discrepancy highlights the influence of processing-induced imperfections during composite fabrication. At higher filler loadings, the resin viscosity increases, which hinders uniform flow and makes it difficult for epoxy to fully impregnate the kenaf fibers. Simultaneously, the available epoxy fraction decreases significantly (from 65 wt.% in C1 to 50 wt.% in C4), reducing the matrix's ability to encapsulate fibers and Cenospheres adequately. Furthermore, Cenospheres tend to agglomerate at higher concentrations, leading to poor dispersion and the entrapment of air pockets during curing. These combined effects contribute to greater porosity in the microstructure.

The presence of such voids is detrimental as they disrupt matrix continuity, diminish the effective load-bearing cross-sectional area, and act as premature crack initiation sites under mechanical loading. While the density reduction achieved through Cenosphere addition is beneficial for lightweight applications, the associated increase in void content emphasizes the need for careful control of filler loading and processing conditions to balance weight reduction with structural integrity.

3.2. Water Absorption and Void Content

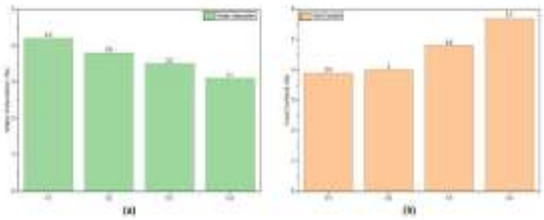

Fig. 7. Variation in (a) water absorption and (b) void content of developed composites

Figure 7 presents the variation in water absorption and void content of the developed composites, revealing an interesting contrast between the two parameters. Water absorption consistently decreased with increasing Cenosphere content, dropping from 4.2% for C1 to 3.1% for C4, even though the void content showed an increasing trend across the same range. At first glance, this observation appears counterintuitive, since higher porosity is typically associated with greater fluid uptake. However, the underlying mechanisms provide a clear explanation. First, the dilution effect plays a major role: kenaf fibers and epoxy, which are relatively hydrophilic in nature, constitute the primary water-absorbing phases of the composite, whereas Cenospheres are chemically inert, hollow, and non-absorbing. With increasing filler content, the relative proportion of hydrophilic phases decreases, resulting in lower overall water uptake. Second, Cenospheres create a barrier effect within the epoxy network. When well-dispersed, they increase the tortuosity of the diffusion pathways available for water molecules, thereby slowing down the ingress of moisture and reducing equilibrium absorption levels. Third, the apparent contradiction between higher void content and reduced water absorption can be explained by void inaccessibility: not all voids formed during composite fabrication are interconnected or open to the surface. Many remain closed pores or correspond to the sealed hollow interiors of Cenospheres, which do not allow water penetration. As a result, despite a higher measured void fraction, only a limited fraction contributes to water uptake. Collectively, these mechanisms demonstrate that the mass dilution and barrier effects of Cenospheres dominate over the contribution from porosity, leading to a net reduction in water absorption with increasing filler addition. This trend is particularly beneficial for improving the dimensional stability and durability of natural fiber composites in humid environments.

3.3. Tensile Strength

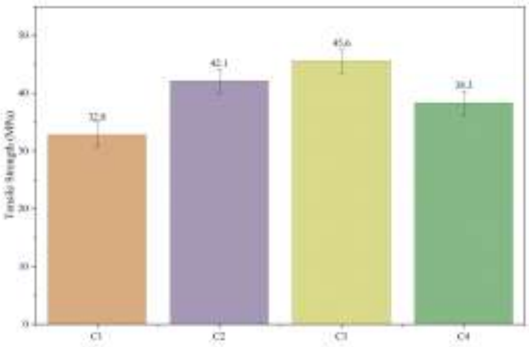

Fig. 8. Variation in tensile strength of developed composites

Figure 8 shows the variation in tensile strength of the developed composites, highlighting a clear improvement with the addition of Cenospheres up to 10 wt.% (C3), followed by a decline at 15 wt.% (C4). The tensile strength increased from 32.8 MPa for the control composite (C1) to a maximum of 45.6 MPa at C3, before reducing to 38.3 MPa at C4. This trend reflects the competing effects of reinforcement and microstructural defects introduced by Cenospheres at different loadings.

The initial improvement from C1 to C3 can be attributed to several synergistic mechanisms. Stress transfer efficiency is enhanced as Cenospheres, being rigid hollow particles, act as secondary reinforcements within the epoxy-rich regions. They help stiffen the matrix and facilitate more efficient stress transfer from the epoxy to the kenaf fibers, thereby improving the composite's load-bearing ability. Additionally, crack bridging and deflection play a key role: the presence of Cenospheres interrupts and redirects propagating cracks, forcing them to take longer and more tortuous paths. This mechanism increases the energy required for fracture and enhances the overall tensile strength. Further, matrix stiffening occurs at moderate filler levels (5–10 wt.%), as Cenospheres reinforce the resin without excessively depleting it. The resin remains sufficient to wet the kenaf fibers adequately, preserving strong fiber–matrix adhesion and ensuring effective load transfer. These combined mechanisms explain the steady rise in tensile strength up to 10 wt.% Cenospheres.

However, at 15 wt.% Cenosphere loading (C4), the tensile strength decreases due to a shift in microstructural balance. The high filler content results in insufficient epoxy to properly impregnate the kenaf fibers, leading to poor fiber wetting and interfacial bonding. This condition promotes fiber pull-out instead of fiber fracture during tensile loading, reducing the composite's strength. Additionally, agglomeration of Cenospheres at higher concentrations introduces weak zones and stress concentration sites, which act as crack initiation points under applied loads. Coupled with this, the increase in void content further reduces the effective load-bearing cross-sectional area, lowering the overall tensile performance.

Thus, the results clearly indicate that 10 wt.% Cenospheres (C3) represent the optimum reinforcement level, where the benefits of stress transfer, crack deflection, and matrix stiffening outweigh the negative effects of resin depletion, clustering, and void formation. Beyond this level, the disadvantages dominate, causing a decline in tensile strength. This confirms that careful control of filler loading is essential to balance mechanical properties in kenaf/Cenosphere/epoxy hybrid composites.

3.4. Flexural Strength

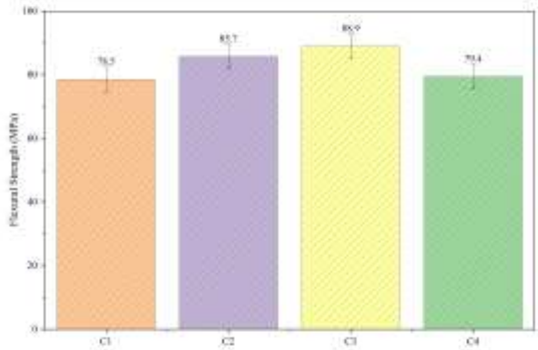

Fig. 9. Flexural strength variation of developed composites

Figure 9 presents the flexural strength variation of the developed composites, which follows a trend similar to that of tensile strength. The flexural strength increased from 78.5 MPa for the neat kenaf/epoxy composite (C1) to a maximum of 88.9 MPa at 10 wt.% Cenosphere loading (C3), before dropping to 79.4 MPa at 15 wt.% Cenosphere addition (C4). The initial improvement up to C3 can be explained by the role of Cenospheres in effectively bearing compressive and tensile stresses generated during bending. In flexural loading, the upper surface of the specimen experiences compressive stresses while the lower surface undergoes tensile stresses. Cenospheres, owing to their rigid and hollow spherical structure, resist these stresses and enhance the stiffness of the composite. Furthermore, their spherical morphology enables uniform redistribution of localized stresses within the epoxy-rich regions, delaying micro-crack initiation and propagation. This synergistic interaction between kenaf fibers (which carry tensile loads) and Cenospheres (which stabilize compressive zones and reduce stress concentration) results in the observed improvement in flexural strength up to 10 wt.% filler loading.

However, beyond this optimum level, specifically at 15 wt.% Cenosphere addition, the flexural performance deteriorates. The decline can be attributed to multiple factors: (i) fiber under-impregnation due to excessive filler presence, which prevents proper wetting of kenaf fibers by the epoxy matrix, thereby reducing stress transfer efficiency, (ii) clustering or agglomeration of Cenospheres, which introduces stress concentration sites, and (iii) higher void content, as indicated by density measurements, which weakens the composite by facilitating early crack initiation under bending stresses. These defects collectively compromise the structural integrity and lead to premature failure under flexural loading. Thus, the flexural results, in agreement with tensile behavior, confirm that 10 wt.% Cenosphere reinforcement (C3) offers the optimum balance between stiffness enhancement and defect minimization, making it the most effective composition for flexural performance.

3.5. *Impact Strength*

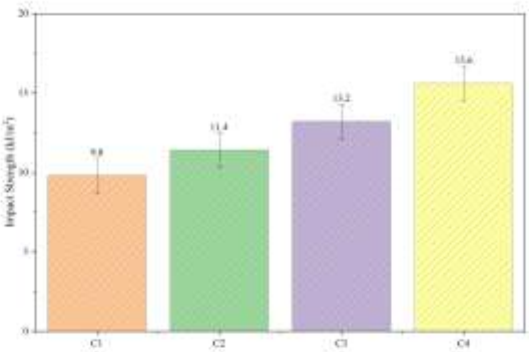

Fig. 10. Impact strength variation of developed composites

Figure 10 illustrates the variation in impact strength of the developed composites, which shows a steady and monotonic increase with rising Cenosphere content, ranging from 9.8 kJ/m^2 for C1 (0 wt.% Cenospheres) to 15.6 kJ/m^2 for C4 (15 wt.% Cenospheres). This behavior is distinct from tensile and flexural strength trends because impact loading is governed by dynamic energy absorption mechanisms, where the ability of the material to resist sudden loads and dissipate kinetic energy determines its performance. The addition of Cenospheres significantly influences these mechanisms by introducing unique failure and energy-dissipation pathways within the kenaf/epoxy system.

One of the primary mechanisms contributing to this increase is particle fracture and debonding. Under high strain-rate loading, hollow Cenospheres fracture or debond from the epoxy matrix. This localized failure dissipates a large amount of energy through micro-cracking and the creation of new fracture surfaces. In addition, the crack deflection and increased tortuosity caused by Cenospheres play a crucial role in enhancing toughness. Instead of propagating along a straight and low-energy path, cracks are forced to deviate and navigate around Cenospheres, increasing the overall fracture surface area and the energy required for crack propagation. This results in a tougher and more impact-resistant composite.

Furthermore, localized plastic deformation of the epoxy matrix around Cenospheres is promoted due to stress concentration at the particle–matrix interface. During impact, these regions undergo micro-yielding, which provides additional energy absorption through matrix plasticity. The presence of kenaf fibers adds to this effect by bridging cracks and delaying catastrophic failure, while Cenospheres introduce discontinuities that increase resistance to rapid crack propagation.

The maximum impact strength at C4 highlights the fact that higher Cenosphere fractions enhance toughness and dynamic energy absorption capacity, despite negatively affecting static properties such as tensile and flexural strength. The reduction in tensile and flexural performance at higher filler loadings can be linked to increased void content, poor interfacial adhesion, and clustering of Cenospheres, which reduce stress transfer efficiency. However, in the case of impact, these same features provide additional sites for energy dissipation, thereby improving toughness.

Thus, the results highlight the dual role of Cenospheres in composite design: while they may compromise stiffness and strength in static loading due to microstructural defects, they significantly enhance toughness and impact resistance under dynamic loading. This underscores the importance of tailoring filler content based on the intended application, where 15 wt.% Cenospheres (C4) offer superior performance for impact-dominated scenarios, while 10 wt.% Cenospheres (C3) may be more suitable for applications requiring higher tensile and flexural strength.

3.6. Comparison with Conventional Glass-Fiber Reinforced Composites

The properties of the developed Cenosphere–kenaf reinforced epoxy composites were compared with conventional glass-fiber reinforced polymer composites to assess their potential for engineering applications. Glass-fiber reinforced composites typically exhibit higher tensile and flexural properties because of the inherently superior strength and stiffness of glass fibers. However, they generally possess densities in the range of approximately 1.8–2.0 g/cm^3, whereas the developed composites exhibited lower densities ranging from 1.15–1.23 g/cm^3.

Although the developed composites may not reach the absolute strength levels of conventional glass-fiber composites, their lower density contributes to improved specific properties and weight reduction benefits. The optimized composite (C3) showed a specific tensile strength of 38.32 MPa·cm^3/g and a specific flexural strength of 74.71 MPa·cm^3/g, demonstrating favourable strength-to-weight characteristics. In addition, the incorporation of renewable kenaf fibers and industrial waste-derived Cenospheres provides environmental benefits that are not typically associated with traditional glass-fiber systems. Therefore, these composites may be promising candidates for lightweight, non-structural, and semi-structural applications in transportation and sustainable mobility sectors.

3.7. Fractography

The SEM images of the composites as presented in Figure 11 reveal microstructural features that strongly correspond to their mechanical performance and physical characteristics. C1 exhibits tensile and flexural fracture surfaces dominated by fiber pull-out, interfacial debonding, and voids, as seen in the SEM micrographs. The matrix appears relatively smooth, indicating brittle failure. This correlates with the low tensile strength (32.8 MPa), moderate flexural strength (78.5 MPa), and the relatively low impact strength (9.8 kJ/m^2).

C3 shows the most balanced properties, with tensile (45.6 MPa) and flexural strengths (88.9 MPa) reaching their peak values, and impact strength increasing to 13.2 kJ/m^2. SEM images indicate strong interfacial bonding, minimal fiber pull-out, and clear evidence of fiber fracture rather than debonding.

C4, with the highest Cenosphere content, exhibits the highest impact strength (15.6 kJ/m^2) as shown by the SEM image of the impact fracture surface, which displays extensive fiber breakage, rough surfaces, and crack branching. These features indicate effective energy dissipation through fiber fracture and matrix shear yielding. However, tensile (38.3 MPa) and flexural (79.4 MPa) strengths decrease compared to C3, likely due to stress concentrations induced by higher void content (5.7%) and reduced density (1.15 g/cm^3 actual), which limit static load-bearing capacity. Water absorption is lowest (3.1%), suggesting that higher filler content reduces the hydrophilic pathways in the composite.

The SEM analysis confirms that C3 achieves the optimal balance of tensile and flexural strength due to strong fiber–matrix interaction, whereas C4 sacrifices some static properties to excel in impact toughness, and C1 consistently shows weak interfacial bonding and brittle fracture, resulting in the lowest performance across mechanical and physical properties.

The interfacial interactions between the epoxy matrix, kenaf fibers, and Cenosphere are presented in Figure 12. They significantly influence the overall composite behaviour. The epoxy matrix transfers applied loads to the reinforcing phases through interfacial adhesion mechanisms. In the case of kenaf fibers, bonding with the epoxy matrix occurs mainly through mechanical interlocking and secondary intermolecular interactions. The hydroxyl groups present in natural fibers may promote hydrogen bonding and improve wettability with the matrix, enabling effective stress transfer.

The interaction between Cenospheres and epoxy primarily occurs through mechanical anchoring and particle–matrix adhesion. Uniformly distributed Cenospheres may act as stress transfer sites and can promote crack deflection and energy dissipation mechanisms. However, excessive filler content may lead to particle agglomeration and void formation, reducing interfacial integrity and causing stress concentration effects.

The combined reinforcing action of kenaf fibers and Cenospheres therefore creates a synergistic effect in which efficient interfacial bonding improves load transfer capability and contributes to enhanced mechanical performance of the developed composites.

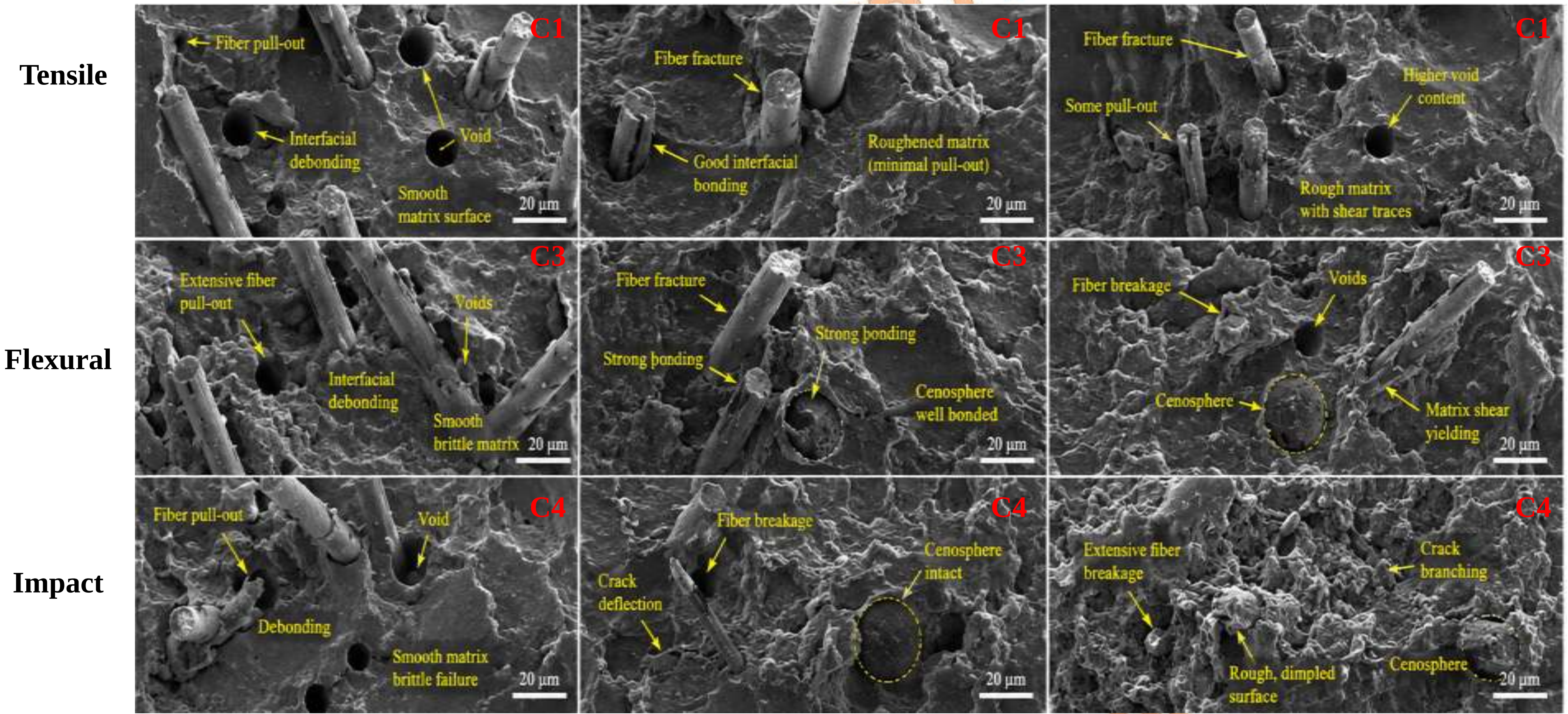

Fig. 11. Fractographic images of samples exhibiting the least and best properties

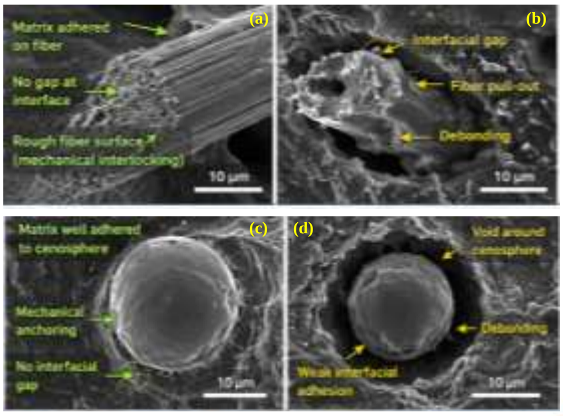

Fig. 12. SEM images showing interfacial interactions between (a)Fiber and epoxy with good bonding; (b)Fiber and epoxy with bad bonding; (c) Cenosphere and epoxy with good bonding, and (d) Cenosphere and epoxy with bad bonding

3.8. MADM-TOPSIS

The composites of various configurations are compared using the TOPSIS method, and each configuration is given a rating depending on the results. Tables 3 and 4 display the decision matrix and the normalized matrix that were created based on the experiments that were conducted, respectively. Using the outcomes of every test for every composite configuration, the decision matrix is created.

Table 3. Decision Matrix

Composite	Tensile Strength (MPa)	Flexural Strength (MPa)	Impact Strength (kJ/m^2)	Actual Density (g/cm^3)	Water Absorption (%)	Void Content (%)
C1	32.8	78.5	9.8	1.23	4.2	3.9
C2	42.1	85.7	11.4	1.21	3.8	4.0
C3	45.6	88.9	13.2	1.19	3.5	4.8
C4	38.3	79.4	15.6	1.15	3.1	5.7

Table 4. Normalized Matrix

Composite	Tensile Strength	Flexural Strength	Impact Strength	Actual Density	Water Absorption	Void Content
C1	0.41	0.47	0.39	0.51	0.57	0.42
C2	0.53	0.51	0.45	0.51	0.52	0.43
C3	0.57	0.53	0.52	0.50	0.48	0.52
C4	0.48	0.48	0.61	0.48	0.42	0.61

The characteristics' weights are determined using the entropy approach, and the results are summarized in Table 5. The weighted normalized matrix is then created using these weights, as indicated in Table 6.

Table 5. Weights calculated from the entropy method

Parameters	Weights (Calculated from Entropy Method)
Tensile Strength	0.17
Flexural Strength	0.03
Impact Strength	0.35
Density	0.01
Water Absorption	0.15
Void Content	0.29

Table 6. Weighted normalised matrix

Composite	Tensile Strength	Flexural Strength	Impact Strength	Actual Density	Water Absorption	Void Content
C1	0.07	0.02	0.14	0.00	0.08	0.12
C2	0.09	0.02	0.16	0.00	0.08	0.12
C3	0.10	0.02	0.18	0.00	0.07	0.15
C4	0.08	0.02	0.22	0.00	0.06	0.18

The positive ideal solution (PIS) and negative ideal solutions (NIS) are calculated and tabulated in Table 7.

Table 7. Positive and negative ideal solutions

	Tensile Strength	Flexural Strength	Impact Strength	Actual Density	Water Absorption	Void Content
PIS	0.10	0.02	0.22	0.00	0.06	0.12
NIS	0.07	0.02	0.14	0.00	0.08	0.18

The composite configurations are ranked according to their relative closeness, separation from the positive ideal solution, and separation from the negative ideal solution, as indicated in Table 8. The configuration with the highest relative closeness is ranked number one, and the configuration with the lowest relative closeness is ranked number four.

Table 8. Relative closeness and ranking

Composite configuration	Separation from PIS	Separation from NIS	Relative Closeness	Ranking
C1	0.09	0.06	0.39	3
C2	0.06	0.06	0.50	2
C3	0.04	0.06	0.59	1
C4	0.06	0.08	0.59	1

According to the TOPSIS research, C3/C4 has the best overall features when compared to C2 and C1, with ranks 1 to C3 and C4, 2 to C2, and 3 to C1.

3.9. Lightweighting Analysis

The lightweighting potential of the developed composites was assessed by comparing their actual densities with those of conventional automotive materials. The calculated weight reduction percentages relative to mild steel and aluminium are presented in Table 9.

Table 9. Weight reduction potential of kenaf–Cenosphere reinforced epoxy composites

Composite	Actual Density (g/cm^3)	Weight Reduction vs Steel (%)	Weight Reduction vs Aluminum (%)
C1	1.23	84.33	54.44
C2	1.21	84.59	55.19
C3	1.19	84.84	55.93
C4	1.15	85.35	57.41

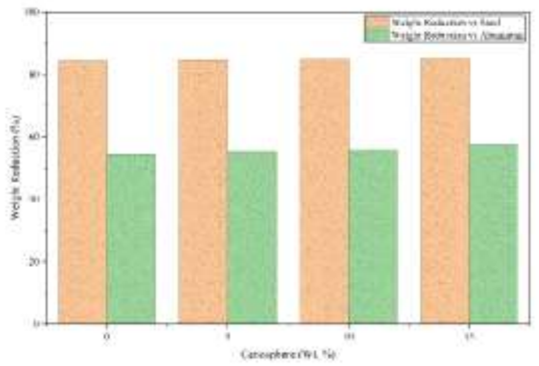

Fig. 12 Weight reduction achieved by kenaf–Cenosphere reinforced epoxy composites relative to conventional steel and aluminum materials

The results presented in Figure 12 reveal a continuous reduction in composite density with increasing Cenosphere content. The density decreased from 1.23 g/cm^3 for C1 to 1.15 g/cm^3 for C4, corresponding to an overall reduction of approximately 6.5%. This reduction can be attributed to the inherently low density and hollow spherical morphology of Cenosphere, which effectively replace a portion of the comparatively denser epoxy matrix.

Relative to mild steel, all composite formulations exhibited exceptional lightweighting potential, achieving weight reductions exceeding 84%. Among the investigated composites, C4 demonstrated the highest reduction of 85.35%, while C1 showed the lowest reduction of 84.33%. Although the numerical differences among the composite formulations appear modest, even small reductions in material density are highly significant in transportation applications where overall vehicle mass directly influences fuel consumption, energy efficiency, and greenhouse gas emissions.

Similarly, when compared with aluminium, which is widely used as a lightweight engineering material in automotive and aerospace sectors, the developed composites achieved weight reductions ranging from 54.44% to 57.41%. The highest reduction was again observed for C4 owing to its lowest density. These values indicate that the developed composites offer a substantial mass advantage over conventional aluminium components while maintaining acceptable mechanical performance.

The observed lightweighting benefits are particularly relevant for sustainable mobility applications. Vehicle mass reduction is directly associated with lower fuel consumption in internal combustion engine vehicles and enhanced driving range in electric vehicles. Previous studies have reported that every 10% reduction in vehicle weight can result in significant improvements in fuel economy and reductions in carbon emissions. Therefore, the combination of low-density, renewable kenaf fibers, and waste-derived Cenospheres makes the developed composites attractive candidates for lightweight automotive interior panels, door trims, dashboard structures, seat back panels, trunk liners, and other semi-structural components.

Among the investigated formulations, C4 exhibited the greatest lightweighting potential due to its lowest density. However, considering the simultaneous requirement for mechanical performance and structural integrity, C3 may represent a more balanced material choice because it combines substantial weight reduction with superior tensile and flexural properties. Consequently, the developed kenaf–Cenosphere reinforced epoxy composites demonstrate considerable promise as sustainable lightweight materials capable of replacing conventional metallic components in automotive applications while contributing to improved energy efficiency and reduced environmental impact.

3.10. Sustainability Assessment

The calculated density reductions relative to the control composite (C1) are presented in Table 10.

Table 10. Density reduction of Cenosphere-filled kenaf/epoxy composites relative to C1

Composite	Actual Density (g/cm^3)	Density Reduction (%)
C1	1.23	0.00
C2	1.21	1.63
C3	1.19	3.25
C4	1.15	6.50

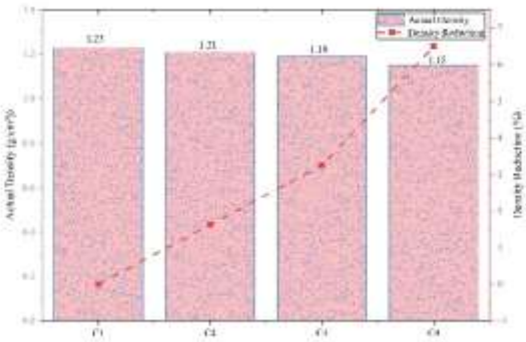

Fig. 13 Reduction in density of composites

The results presented in Figure 13 indicate a progressive decrease in composite density with increasing Cenosphere content. Compared with the control composite, density reductions of 1.63%, 3.25%, and 6.50% were achieved for C2, C3, and C4, respectively. This behaviour is primarily attributed to the hollow spherical morphology and inherently low density of Cenospheres, which replace a portion of the relatively denser epoxy matrix.

The observed reduction in density is particularly beneficial from a sustainability perspective because lighter materials require less raw material per unit volume and contribute directly to vehicle weight reduction. Consequently, the use of higher Cenosphere loadings offers a dual advantage of reducing both material consumption and component mass.

An important sustainability advantage of the developed composites is the incorporation of Cenospheres, which are waste-derived aluminosilicate microspheres generated during coal combustion processes in thermal power plants. Large quantities of Cenospheres are typically disposed of in ash ponds or landfills, creating environmental and land management challenges.

The utilization of Cenospheres as reinforcement in polymer composites converts an industrial waste stream into a value-added engineering material. Such waste valorisation supports circular economy principles by extending the lifecycle of industrial by-products and reducing the demand for virgin mineral fillers. Furthermore, replacing a portion of the epoxy matrix with Cenospheres lowers the overall consumption of petroleum-derived polymer resin, thereby reducing the environmental footprint of the composite manufacturing process.

As Cenosphere loading increased from 0 wt.% in C1 to 15 wt.% in C4, the amount of industrial waste incorporated into the composite increased proportionally, thereby enhancing the sustainability profile of the material system.

The incorporation of kenaf fibers further enhances the environmental sustainability of the developed composites. Kenaf is a rapidly renewable lignocellulosic fiber that can be cultivated within a relatively short growth cycle, making it an attractive alternative to conventional synthetic reinforcements. Compared with materials such as glass fibers, kenaf requires substantially lower energy inputs during cultivation, processing, and manufacturing, resulting in a reduced embodied carbon footprint. The incorporation of 35 wt.% kenaf fiber in all composite formulations contributes to a decreased reliance on non-renewable synthetic reinforcements, lower energy consumption during raw material production, and reduced greenhouse gas emissions associated with material processing. Furthermore, the natural origin of kenaf improves the end-of-life sustainability of the composite system through partial biodegradability and enhanced environmental compatibility. Consequently, the synergistic combination of renewable kenaf fibers and waste-derived Cenospheres offers an environmentally responsible and resource-efficient approach for the development of sustainable composite materials suitable for lightweight transportation and mobility applications.

A comparative sustainability assessment was performed based on three key criteria: density reduction and lightweighting potential, utilization of industrial waste-derived Cenospheres, and renewable reinforcement content. Since all composite formulations contained a constant kenaf fiber content of 35 wt.%, the primary variation in sustainability performance arose from the increasing incorporation of Cenospheres and the corresponding reduction in composite density. Based on these considerations, the sustainability ranking of the developed composites was established as C4 > C3 > C2 > C1. The superior sustainability performance of C4 is attributed to its highest Cenosphere loading, which resulted in the maximum density reduction, lowest material consumption per component, and greatest utilization of industrial waste resources. In contrast, C1 exhibited the lowest sustainability performance because it contained no Cenosphere reinforcement and relied more heavily on epoxy resin, a petroleum-derived material. The results clearly indicate that increasing Cenosphere content enhances the sustainability profile of kenaf–epoxy composites by simultaneously promoting lightweighting and waste valorization. Consequently, the combined use of renewable kenaf fibers and waste-derived hollow Cenospheres represents a promising strategy for developing environmentally sustainable composite materials suitable for next-generation lightweight automotive and mobility applications.

3.11. Suitability of Developed Composite for Sustainable Mobility Applications

The specific properties of the developed composites are provided in Table 11.

Table 11. Specific properties of developed composites

Composite	Specific Tensile Strength ($MPa \cdot cm^3/g$)	Specific Flexural Strength ($MPa \cdot cm^3/g$)	Specific Impact Strength ($kJ \cdot m^{-2} \cdot cm^3/g$)
C1	26.67	63.82	7.97
C2	34.79	70.83	9.42
C3	38.32	74.71	11.09
C4	33.30	69.04	13.57

The applicability of the developed Cenosphere–kenaf reinforced epoxy composites for sustainable mobility applications was quantitatively assessed using density reduction and specific mechanical properties (property-to-density ratio). Lightweight materials with high specific properties are preferred in automotive and transportation sectors because lower structural weight contributes to reduced fuel consumption and improved energy efficiency.

The actual density of the composites progressively decreased from 1.23 g/cm^3 for C1 to 1.15 g/cm^3 for C4, representing an approximate 6.5% reduction in weight. This reduction indicates the beneficial contribution of low-density Cenosphere fillers toward lightweight structural development.

To evaluate structural efficiency, specific mechanical properties were calculated by normalizing the mechanical properties with composite density. The specific tensile strength increased from 26.67 $MPa \cdot cm^3/g$ (C1) to 38.32 $MPa \cdot cm^3/g$ (C3), corresponding to an approximately 43.7% improvement. Similarly, the specific flexural strength increased from 63.82 $MPa \cdot cm^3/g$ (C1) to 74.71 $MPa \cdot cm^3/g$ (C3), showing an approximately 17.1% enhancement. Furthermore, the specific impact strength increased from 7.97 $kJ \cdot m^{-2} \cdot cm^3/g$ (C1) to 13.57 $kJ \cdot m^{-2} \cdot cm^3/g$ (C4), resulting in an approximately 70.3% improvement.

The improved specific properties indicate that the developed composites provide enhanced mechanical efficiency while maintaining reduced density. Such characteristics are desirable for lightweight structural and semi-structural components in sustainable mobility systems, where improved strength-to-weight and impact-to-weight performance can contribute to enhanced energy efficiency and reduced environmental impact.

4. Applications, Advantages, Limitations and Future Work Directions

The developed Cenosphere–kenaf reinforced epoxy composites demonstrate strong potential for application in automotive and transportation sectors, particularly in non-structural and semi-structural components where lightweight materials are essential. The reduction in density combined with improved specific mechanical performance makes these composites suitable for applications aimed at enhancing fuel efficiency and reducing overall vehicle weight. In addition, the use of renewable kenaf fibers and industrial waste-derived Cenospheres supports sustainability objectives by promoting resource efficiency, waste valorisation, and reduced dependence on conventional synthetic reinforcements.

From an economic perspective, the proposed composite system offers favourable potential due to the low cost and wide availability of kenaf fibers and Cenospheres. However, successful large-scale implementation requires careful control of processing parameters to ensure uniform filler dispersion, consistent fiber–matrix interaction, and repeatable manufacturing quality, along with consideration of production economics.

Despite these advantages, several limitations must be acknowledged. Natural fiber-based composites such as kenaf-reinforced systems are prone to moisture absorption due to the hydrophilic nature of the fibers, which can adversely affect dimensional stability and long-term mechanical performance under humid or variable environmental conditions. In addition, epoxy matrices exhibit relatively limited thermal resistance compared to metallic materials, which may restrict their application in high-temperature zones of automotive structures. At higher Cenosphere loadings, the possibility of particle agglomeration and interfacial defects increases, which may negatively influence impact resistance and fatigue behaviour under cyclic loading. Furthermore, issues such as recyclability, long-term durability, and performance under real service conditions involving vibration, UV exposure, and thermal cycling remain critical concerns.

In this context, moisture-induced degradation of kenaf fibers, including fiber swelling and interfacial weakening, is a key factor influencing long-term durability. Surface modification techniques and coupling agents may be employed to reduce moisture sensitivity and improve fiber–matrix adhesion, thereby enhancing environmental stability.

Although the present study evaluated key properties such as density, water absorption, tensile, flexural, and impact strength (with impact strength improving from 9.8 kJ/m^2 for C1 to 15.6 kJ/m^2 for C4, corresponding to a 59.2% increase), additional performance characteristics were not investigated. In particular, fatigue behaviour and long-term environmental aging remain essential for assessing real-world reliability. Environmental factors such as moisture uptake, thermal cycling, UV exposure, and cyclic mechanical loading may significantly influence long-term performance.

Therefore, future research should focus on fatigue analysis under cyclic loading, environmental aging under varying humidity and temperature conditions, UV resistance, thermal cycling effects, and moisture-induced degradation mechanisms. Additionally, retention of mechanical properties after prolonged exposure and microstructural characterization of degradation mechanisms will be essential to establish long-term durability and service life. Such studies will provide a more comprehensive understanding of the applicability of these composites in real transportation environments.

5. Conclusions

Kenaf and Cenosphere-based hybrid composites fabricated via hand lay-up and compression moulding revealed that the interplay of natural fibers and hollow fillers governs their structural efficiency, lightweighting capability, sustainability, and impact energy absorption. The incorporation of Cenospheres progressively reduced the theoretical density of the composites from 1.28 g/cm^3 (C1) to 1.22 g/cm^3 (C4), corresponding to a 4.7% reduction, while the actual density decreased by 6.5% across the same range. This decrease was accompanied by an increase in void content from 3.9% to 5.7% (a 46.2% rise), indicating higher porosity with greater filler loading. Interestingly, water absorption exhibited the opposite trend, declining from 4.2% (C1) to 3.1% (C4), signifying a 26.2% improvement in moisture resistance.

The mechanical properties revealed a distinct balance between strength and toughness. Tensile strength improved from 32.8 MPa (C1) to a maximum of 45.6 MPa at C3 (a 39% increase), before decreasing to 38.3 MPa at C4, which nevertheless remained 16.8% higher than the baseline. Flexural strength followed a similar trend, increasing from 78.5 MPa (C1) to 88.9 MPa at C3 (13.2% rise) before reducing to 79.4 MPa at C4. In contrast, impact strength increased continuously from 9.8 kJ/m^2 in C1 to 15.6 kJ/m^2 in C4, representing a 59.2% enhancement. Overall, C3 emerged as the optimum composition offering the best balance of tensile and flexural performance, whereas C4 maximized impact resistance, making it suitable for applications where energy absorption is prioritized over load-bearing capability.

The lightweighting analysis demonstrated the significant potential of the developed composites as alternatives to conventional metallic materials in transportation applications. Compared with mild steel, the composites achieved weight reductions ranging from 84.33% to 85.35%, while reductions of 54.44% to 57.41% were obtained relative to aluminium. The lowest-density formulation, C4 (1.15 g/cm^3), exhibited the highest lightweighting potential, highlighting the effectiveness of Cenospheres in reducing component mass and enhancing fuel efficiency and vehicle range.

From a sustainability perspective, the incorporation of Cenospheres improved the environmental profile of the composites by utilizing waste-derived hollow microspheres generated from thermal power plants and reducing dependence on petroleum-based epoxy resin. Furthermore, the use of 35 wt.% renewable kenaf fibers contributed to lower embodied energy, reduced greenhouse gas emissions, and improved end-of-life sustainability compared with conventional synthetic reinforcements. The sustainability assessment ranked the formulations as C4 > C3 > C2 > C1, owing to the increasing utilization of industrial waste and progressive density reduction with higher Cenosphere loading.

SEM analysis confirmed the strong correlation between microstructural features and composite performance. C1 exhibited poor interfacial bonding and brittle fracture characteristics, resulting in the lowest strength and toughness. C3 achieved the most effective fiber–matrix interaction, leading to peak tensile (45.6 MPa) and flexural (88.9 MPa) strengths together with enhanced impact resistance (13.2 kJ/m^2). C4 displayed the highest impact toughness (15.6 kJ/m^2) and lowest water absorption (3.1%), but experienced a reduction in static mechanical properties due to increased void content and localized stress concentrations associated with higher Cenosphere loading.

The TOPSIS-based multi-attribute decision-making analysis further validated the overall performance of the developed composites. The relative closeness values indicated that C3 (0.59) and C4 (0.59) were the most preferred formulations, followed by C2 (0.50) and C1 (0.39). While C4 delivered superior lightweighting, sustainability, and impact performance, C3 provided the most balanced combination of mechanical strength, cost efficiency, structural integrity, and weight reduction. Therefore, C3 is recommended as the optimum composite for lightweight automotive interior and semi-structural applications, whereas C4 is more suitable for impact-dominated and energy-absorbing components where maximum lightweighting and sustainability benefits are desired. The results demonstrate that the synergistic integration of renewable kenaf fibers and waste-derived Cenospheres offers a viable pathway for developing sustainable composite materials capable of supporting next-generation mobility systems.

The developed kenaf–Cenosphere epoxy composites show strong potential for sustainable mobility applications due to their reduced density, improved specific mechanical properties, and environmental benefits. Their lightweight nature can contribute to improved fuel efficiency and reduced emissions in transportation systems. In addition, the use of renewable kenaf fibers and waste-derived Cenospheres supports sustainability through resource efficiency and waste valorization, making them suitable for non-structural and semi-structural automotive components.

Acknowledgement

The authors acknowledge the CAMRA Laboratory, Department of IEM, Siddaganga Institute of Technology, Tumakuru, and the Research Centre of the Department of IEM, Siddaganga Institute of Technology, Tumakuru for providing the necessary facilities to carry out the study.

Funding Statement

This research did not receive any specific grant from funding agencies in the public, commercial, or not-for-profit sectors.

Conflicts of Interest

The author declares that there is no conflict of interest regarding the publication of this article.

References

[1] Al-Oqla, F.M. and Salit, M.S., 2017. Materials Selection for Natural Fiber Composites. United Kingdom: Woodhead Publishing.

[2] Pai, Y., Pai, K.D. and Kini, M.V., 2023. Effect of ageing conditions on the low velocity impact behavior and damage characteristics of aramid-basalt/epoxy hybrid interply composites. Engineering Failure Analysis, 152, p.107492.

[3] Kumar, S., Varadarajan, Y.S. and Shamprasad, M.S., 2023. Three-body abrasive wear behavior of rice straw fibers reinforced PLA composites. Materials Today: Proceedings, 92, pp.322–326.

[4] Mahesh, V., 2023. Development and ballistic impact study on environment friendly sustainable jute reinforced carbon black/lignin-based elastomeric flexible composites. Proceedings of the Institution of Mechanical Engineers, Part L: Journal of Materials: Design and Applications.

[5] Mahesh, V., 2023. Study on slurry erosion resistance and damage mechanism in cenosphere reinforced syntactic foams for lightweight applications. International Journal of Lightweight Materials and Manufacture.

[6] Bax, B. and Müssig, J., 2008. Impact and tensile properties of PLA/Cordenka and PLA/flax composites. Composites Science and Technology, 68(7–8), pp.1601–1607.

[7] Vishwas, M., Vinyas, M. and Puneeth, K., 2020. Influence of areca nut nanofiller on mechanical and tribological properties of coir fibre reinforced epoxy-based polymer composite. Scientia Iranica, 27(4), pp.1972–1981.

[8] Aithal, N.U., Mahesh, V. and Mahesh, V., 2023. Harnessing of waste cenosphere in development of natural/synthetic and rubber core sandwich composite and its mechanical characterization. Biomass Conversion and Biorefinery, 14, pp.25057–25069.

[9] Mahesh, V.V., et al., 2022. Comparative study on energy absorbing behavior of stiff and flexible composites under low velocity impact. Materials Today: Proceedings.

[10] Mahesh, V., Mahesh, V. and Harursampath, D., 2022. Physio-mechanical characterization of jute/Kevlar hybrid composites coupled with MADM approach for selection of composites. Journal of Natural Fibers, 19(15), pp.11105–11113.

[11] Kumbhare, K.S., Mahesh, V., Joladarashi, S. and Kulkarni, S.M., 2022. Comparative study on low velocity impact behavior of natural hybrid and non-hybrid flexible thermoplastic based composites. Journal of Thermoplastic Composite Materials.

[12] R., N.S., et al., 2023. Isolation and characterization of agro-waste biomass sapodilla seeds as reinforcement in potential polymer composite applications. Heliyon, 9(7), e17760.

[13] Ebrahimnezhad-Khaljiri, H., Eslami-Farsani, R., Najafi, M. and Saeedi, A., 2022. Introduction to epoxy/natural fiber composites. In: S.M. Rangappa, J. Parameswaranpillai, S. Siengchin and S. Thomas, eds. Handbook of Epoxy/Fiber Composites. Singapore: Springer Nature, pp.485–514.

[14] Saeedi, A., Eslami-Farsani, R., Ebrahimnezhad-Khaljiri, H. and Najafi, M., 2020. Dynamic mechanical analysis of epoxy/natural fiber composites. In: S.M. Rangappa, J. Parameswaranpillai, S. Siengchin and S. Thomas, eds. Handbook of Epoxy/Fiber Composites. Singapore: Springer, pp.1–28.

[15] R., N.S., et al., 2024. Enhanced thermal and mechanical properties of sapodilla/PLA biocomposites using filament extrusion 3D printing. Functional Composites and Structures, 6(4), 045014.

[16] Wambua, P., Ivens, J. and Verpoest, I., 2003. Natural fibres: Can they replace glass in fibre reinforced plastics? Composites Science and Technology, 63(9), pp.1259–1264.

[17] Mohammed, I., Talib, A.R.A., Sultan, M.T.H., Jawaid, M., Ariffin, A.H. and Saadon, S., 2018. Mechanical properties of fibre-metal laminates made of natural/synthetic fibre composites. BioResources, 13(1), pp.2022–2034.

[18] Murugadoss, P., et al., 2025. Kenaf/basalt fiber-reinforced epoxy matrix hybrid composites: Current trends, challenges, and future prospects in advanced material development. Results in Engineering, 26, 104816.

[19] Mahesh, V., Mahesh, V., Harursampath, D., Joladarashi, S. and Kulkarni, S.M., 2022. Development of sustainable jute/epoxy composite and assessing the effect of rubber crumb on low velocity impact response. Journal of Natural Fibers, pp.1–12.

[20] Mahesh, V., Joladarashi, S. and Kulkarni, S.M., 2019. An experimental study on adhesion, flexibility, interlaminar shear strength, and damage mechanism of jute/rubber-based flexible 'green' composite. Journal of Thermoplastic Composite Materials, pp.1–28.

[21] Huang, Y., Sultan, M.T.H., Shahar, F.S., Łukaszewicz, A., Oksiuta, Z. and Grzejda, R., 2025. Kenaf fiber-reinforced biocomposites for marine applications: A review. Materials, 18(5), 999.

[22] Mahesh, V., 2023. Statistical approach of determining the effect of cenosphere on the tribological behaviour of jute reinforced polymer based composite. Mechanics of Advanced Composite Structures, 10(1), pp.211–220.

[23] Suresha, B., Chandramohan, G., Siddaramaiah and Jayaraju, T., 2008. Influence of cenosphere filler additions on the three-body abrasive wear behavior of glass fiber-reinforced epoxy composites. Polymer Composites, 29(3), pp.307–312.

[24] Hegde, S., Padmaraj, N.H., Siddesh, V., Sunaya, T.S., Kini, K.A. and Sanil, V.K., 2021. Experimental investigation of mechanical sustainability and acoustic performance of fly ash cenosphere/epoxy polymer composites. Journal of King Saud University – Engineering Sciences.

[25] Atul Ltd. Polymer Division, 2020. Technical Data Sheet: Lapox L-12 Resin and K-6 Hardener. Atul Ltd., Polymer Division.

[26] Flynn, J., Amiri, A. and Ulven, C., 2016. Hybridized carbon and flax fiber composites for tailored performance. Materials & Design, 102, pp.21–29.

[27] Begum, K. and Islam, M., 2013. Natural fiber as a substitute to synthetic fiber in polymer composites: A review. Research Journal of Engineering Sciences, 2, pp.46–53.

[28] Supian, A.B.M., et al., 2024. Kenaf/glass fiber-reinforced polymer composites: Pioneering sustainable materials with enhanced mechanical and tribological properties. Polymer Composites, 45(16), pp.14421–14447.

[29] Chiner, M., 1988. Planning of expert systems for materials selection. Materials & Design, 9(4), pp.195–203.

[30] Karana, E., Hekkert, P. and Kandachar, P., 2008. Material considerations in product design: A survey on crucial material aspects used by product designers. Materials & Design, 29(6), pp.1081–1089.

[31] Mehmood, Z., Haneef, I. and Udrea, F., 2018. Material selection for micro-electro-mechanical systems (MEMS) using Ashby's approach. Materials & Design, 157, pp.412–430.

[32] Kolios, A., Mytilinou, V. and Lozano-Minguez, E., 2016. A comparative study of multiple-criteria decision-making methods under stochastic inputs. Energies, 9(7), p.566.

[33] Behzadian, M., Otaghsara, S.K., Yazdani, M. and Ignatius, J., 2012. A state-of-the-art survey of TOPSIS applications. Expert Systems with Applications, 39(17), pp.13051–13069.